

# Early triple negative breast cancers in a Singapore cohort exhibit high PIK3CA mutation rates associated with low PD-L1 expression

**Joe Yeong**

Singapore General Hospital

**Denise Goh**

Agency of Science, Technology and Research (A\*STAR)

**Tira J. Tan**

Duke-NUS Medical School

**Benedict Tan**

Agency for Science, Technology and Research (A\*STAR)

**Huren Sivaraj**

National Cancer Centre Singapore

**Valerie Koh**

Singapore General Hospital

**Jeffrey Chun Tatt Lim**

Agency for Science, Technology and Research (A\*STAR)

**Craig Ryan Joseph**

Agency for Science, Technology and Research (A\*STAR)

**Timothy Kwang Yong Tay**

Singapore General Hospital

**Jiangfeng Ye**

Agency for Science, Technology and Research (A\*STAR)

**Mai Chan Lau**

Agency for Science, Technology and Research (A\*STAR)

**Jason Yongsheng Chan**

National Cancer Centre Singapore, National University of Singapore

**Jabed Iqbal**

Singapore General Hospital

**Cedric Chuan Young Ng**

National Cancer Centre Singapore

**Bin Tean Teh**

National Cancer Centre Singapore <https://orcid.org/0000-0003-1514-1124>

**Rebecca Alexandra Dent**

National Cancer Centre Singapore



**Puay Hoon Tan** (✉ [tan.puay.hoon@sgh.com.sg](mailto:tan.puay.hoon@sgh.com.sg))

**Article**

**Keywords:**

**Posted Date:** August 5th, 2022

**DOI:** <https://doi.org/10.21203/rs.3.rs-1876811/v1>

**License:**   This work is licensed under a Creative Commons Attribution 4.0 International License. [Read Full License](#)

---

# Abstract

Mutations in the PI3K pathway, particularly of *PIK3CA*, were reported to be intimately associated with triple negative breast cancer (TNBC) progression and development of treatment resistance. We profiled *PIK3CA* and other genes on 166 early-stage TNBC tumors from Singapore, for comparison to publicly available TNBC cohorts. These tumors were profiled transcriptionally using a Nanostring panel of immune genes and multiplex immunohistochemistry, then manually scored for PD-L1-positivity using two clinically relevant clones, SP142 and 22C3. We discovered a higher rate of *PIK3CA* mutations in our TNBC cohort as compared to non-Asian cohorts, along with *TP53*, *BRCA1*, *PTPN11*, and *MAP3K1* alterations. *PIK3CA* mutations did not affect overall or recurrence-free survival, and when compared to *PIK3CA*<sup>WT</sup> tumors, there were no differences in immune infiltration. Using two clinically approved antibodies, *PIK3CA*<sup>mut</sup> tumors were associated with PD-L1 negativity. Analysis of co-mutation frequencies further revealed that *PIK3CA* mutations tended to be accompanied by MAP kinase pathway mutation. The mechanism and impact of *PIK3CA* alterations on the TNBC tumor immune microenvironment and PD-L1 positivity warrant further study.

## Introduction

Breast cancer is the most prevalent malignant disease (1) and the second major cause of cancer-related deaths in women worldwide (2). Amongst all subtypes, triple negative breast cancer (TNBC) is known to be one of the most aggressive and heterogeneous forms of the disease; it generally occurs at a younger age and is often accompanied by progressive disease, high metastatic and recurrence rates, high-grade histology, and distinctly poor prognosis (3–5). TNBCs are defined by an absence of estrogen receptors (ERs) and progesterone receptors (PRs), as well as a lack of human epidermal growth factor receptor 2 (HER2) overexpression or amplification (2, 6); it is known to be a heterogeneous group of diseases. A previous report described five clinically relevant subtypes that do not involve sophisticated gene expression profiling techniques (7). In particular, TNBC with *AKT/PIK3CA/PTEN* alterations is a clinically relevant subtype, with continuous efforts made to develop inhibitors that target this pathway.

Although there have been therapeutic advances in managing early-stage TNBC in recent years with regards to the use of immune checkpoint blockade with chemotherapy, biomarkers which can inform optimal therapeutic strategies remain elusive. Moreover, the high relapse rate of high risk, residual TNBC represents a critical unmet need (8, 9). Thus, it is crucial to have a deeper understanding of the molecular underpinnings of TNBC, as well as the associated immune responses within the tumor microenvironment to refine patient selection.

The PI3K signalling pathway controls a variety of cellular processes, such as metabolism, proliferation, and apoptosis, and contributes to tumor development and progression (10). Phosphatidylinositol-4,5-bisphosphate 3-kinase catalytic subunit alpha (*PIK3CA*) gene mutations are common in primary breast cancers and are frequently found in the hormone-receptor-positive subtypes (11, 12). These mutations are most often found in the helical (p.E542K and p.E545K in exon 10) and kinase (p.H1047R in exon 21) domains of the *PIK3CA* protein (13). A meta-analysis review of 10,319 early-stage breast cancer patients from 19 studies found that the rates of *PIK3CA* mutation occurrence in TNBC (ER<sup>-</sup>/HER2<sup>-</sup>) were 18%, and that it is significantly associated with favorable invasive disease-free survival, distant disease-free survival, and overall survival among early-stage breast cancers (14).

Dysregulation of PI3K signaling is highly associated with the development of resistance to current standard-of-care treatments in breast cancer patients; in TNBC, PI3K dysregulation is associated with chemotherapy resistance (15). PI3K/AKT signaling is an important target of the PD-1 downstream pathway, where oncogenic PI3K/AKT pathway is reportedly associated with primary resistance to PD-1/PD-L1 checkpoint inhibition (16). Considering the importance of PD-1/PD-L1 and immune-associated pathways in determining the clinical outcomes of TNBC and with recent approvals for the use of immune checkpoint blockade in combination with chemotherapy in early TNBCs (6, 17–19), we aim to characterize alterations in the PI3K/AKT/mTOR pathway in our cohort of Singapore TNBCs and to evaluate the associations of *PIK3CA* mutations with their immune microenvironment. Here, we used multimodal methodologies, including comprehensive genomic profiling, conventional pathology techniques, multiplex immunohistochemistry staining, and NanoString technology to retrospectively evaluate gene alterations, total immune infiltrates, and PD-L1 scoring in primary TNBC tumors, and we further tested our conclusions with a smaller validation cohort.

## Methods

***Clinical and demographic data, and data retrieval from public datasets.*** Clinical and demographic data for Singapore General Hospital discovery (SGH; n = 117) and validation (SGHv; n = 49) cohorts were obtained from patients' medical records. Tumors were typed, staged and graded according to the World Health Organization, American Society of Clinical Oncology-College of American Pathologists (ASCO-CAP) guidelines (20).

Gene expression, clinical, and somatic mutational data were obtained from various databases of publicly available cohorts. Data for the Molecular Taxonomy of Breast Cancer International Consortium (METABRIC) cohort (21) were obtained from cBioportal (project ID: BRCA\_METABRIC) and filtered for TNBC patients on the basis of ER, PR, and HER2 status (n = 292). Data for The Cancer Genome Atlas (TCGA) non-Asian cohort (12) were obtained from Genomic Data Commons (project ID: TCGA-BRCA) and filtered for TNBCs based on ER and PR status and HER2 status, as assessed by fluorescent *in situ* hybridization and immunohistochemistry (IHC) (n = 129). Data for the Fudan University Shanghai Cancer Center (FUSCC) cohort (22) were obtained from BioSino (project ID: OEP000155) (n = 276). A complete demographic summary of the various cohort is detailed in Supplementary table 1.

Disease-free survival and overall survival were defined as the period from the date of diagnosis to the date of recurrence or death, respectively, or to the date of the last follow-up if recurrence or death were not encountered.

***Comprehensive genomic profiling.*** Comprehensive genomic profiling (CGP) was performed on DNA extracted from formalin-fixed, paraffin-embedded (FFPE) samples (FoundationOne®, Cambridge, MA, USA). The CGP sequencing methods used have been validated and reported previously (23). Approximately 50 ng of DNA were extracted from tumor samples and assayed using adaptor ligation and hybrid capture next-generation sequencing (FoundationOne®) for all coding exons from 315 cancer-related genes and selected introns from 28 genes often implicated in cancer (24). The sequencing of captured libraries was performed using Illumina HiSeq technology to a mean exon coverage depth of >500X, and the subsequent sequences were analyzed using both an algorithmic pipeline and manual curation for base substitutions, small insertions or deletions, copy number alterations (focal amplifications and homozygous deletions), and select gene fusions, as described previously (24).

**Ampliseq targeted sequencing.** Targeted sequencing of *PIK3CA* by Qiaseq was performed on DNA extracted from FFPE samples using the probe list provided in Supplementary Table 2. For each sample, DNA was extracted from 8 x 10um FFPE sections using the QIAamp DNA FFPE Kit (Qiagen), following the manufacturer's protocol. The DNA samples were quantified using the Qubit dsDNA High Sensitivity Assay. FFPE repair was then performed using the NEBNext FFPE DNA Repair Mix, following the manufacturer's protocol. For each sample, about 100ng of DNA was used for library construction using the QIAseq Targeted DNA Panel Kit, following the manufacturer's recommendations. Target enrichment was carried out using a customised QIAseq panel comprising of 18 extensively curated genes (Supplementary Table 3). The quality of the libraries was assessed using Agilent's High Sensitivity DNA TapeStation System and quantified using Qubit dsDNA High Sensitivity Assay. The libraries were sequenced with a 2x150 bp configuration on the NovaSeq6000 platform at a minimum sequencing depth of 500X.

**Biocomputational analysis.** FastQC [<https://www.bioinformatics.babraham.ac.uk/projects/fastqc/>] software package was utilized to perform quality checking of the FASTQ sequence files. After removing adapters using trimmomatic (25), trimmed paired reads were mapped to hg19 (hs37d5) using BWA-MEM (v0.7.15-r1140) (26) and sorted/indexed with samtools (27). FreeBayes (v1.1.0-4-gb6041c6, settings: -m 30 -q 30 -F 0.01 -u) (28) and Variant Effect Predictor (VEP) (29) was utilized to call and annotate variants, respectively. Annotated variants were first filtered according to a few criteria: (i) only variants with more than 100X coverage and variant allele frequency of at least 5% were retained; (ii) minor allele frequency of the variant in the normal population must be zero; (iii) synonymous and non-exonic variants were also excluded, and (iv) variants in dbSNP (30) were excluded, unless they are in COSMIC (31) or ClinVar (32). Manual curation of variants passing these filters was done on the Integrative Genomics Viewer (33).

**RNA extraction and NanoString measurement of immune-associated genes.** RNA was extracted from unlabeled FFPE tissue sections (10-µm thick) using a RNeasy FFPE kit (Qiagen, Hilden, Germany) on a QIAcube automated sample preparation system (Qiagen), and it was quantified using an Agilent 2100 Bioanalyzer system (Agilent Technologies, Santa Clara, CA, USA). A total of 100 ng of functional RNA (>300 nucleotides) was assayed on the nCounter MAX Analysis System (NanoString Technologies, Inc., Seattle, WA, USA). The NanoString counts were normalized using positive control probes and housekeeping genes, as previously reported (34, 35). The count data were then logarithmically transformed prior to further analysis.

**Immunohistochemistry.** FFPE tissue sections (4 µm thick) were labelled with two different anti-PD-L1 clones (SP142 and 22C3). The antibody clones were scored separately (0% to 100%), based on combined positive score (CPS), tumor proportion score (TPS) and immune count (IC), as previously described (36-38). CPS is defined as the percentage of total PD-L1<sup>+</sup> cells (tumor cells and immune cells) divided by the total number of tumor cells. TPS is defined as the percentage of tumor cells with membranous PD-L1 expression. IC is defined as the proportion of tumor area occupied by PD-L1<sup>+</sup> tumor-infiltrating immune cells. Tissue sections from patients were labelled to allow the quantification of CPS, TPS and IC. To generate the scores, images of labelled slides were captured using an IntelliSite Ultra-Fast Scanner (Philips Research, Eindhoven, the Netherlands) prior to examination by pathologists.

**Multiplex immunohistochemistry.** Multiplex IHC (mIHC) was performed using an Opal Multiplex IHC kit (Akoya Biosciences, CA, USA) as previously described (17, 39, 40). In brief, FFPE tissue sections were cut onto Bond Plus slides (Leica Biosystems, Richmond, USA) and heated at 60°C for 20 min (6). The tissue sections were then

subjected to deparaffinization, rehydration, and heat-induced epitope-retrieval using a Leica Bond Max autostainer (Leica Biosystems, Melbourne, Australia) before endogenous peroxidase blocking (Leica Biosystems, Newcastle, UK). Next, the slides were incubated with primary antibodies followed by incubation with polymeric HRP-conjugated secondary antibodies (Leica Biosystems, Newcastle, UK) (Supplementary Table 4). Then, the samples were incubated with Opal fluorophore-conjugated tyramide signal amplification (TSA) (Akoya Biosciences) at a 1:100 dilution. The slides were rinsed with wash buffer (BOND Wash Solution 10X concentrate) after each step. Following TSA deposition, the slides were again subjected to heat-induced epitope-retrieval to strip the tissue-bound primary/secondary antibody complexes prior to further labelling. These steps were repeated until the samples were labelled with all six markers and stained with spectral DAPI (Akoya Biosciences) at a 1:10 dilution. Finally, the slides were mounted using ProLong Diamond Anti-fade Mountant (Molecular Probes, Life Technologies, USA) and developed in the dark at room temperature for 24 h. Images of viable tumor regions selected by pathologists were captured for each case under a Vectra 3 pathology imaging system microscope (Akoya Biosciences). Immune cells were classified as intra-tumoral or stromal tumor infiltrating lymphocytes (iTILs and sTILs, respectively) as previously described (19, 38, 41, 42). The mIHC images were scored by a pathologist using inForm software (version 2.4.2; Akoya Biosciences), cellXpress software (43) and HALO™ (Indica Lab).

**Statistical analyses and data visualization.** Statistical analyses were performed in Python (version 3.8) using the numpy (version 1.18), scipy (version 1.3), and statsmodels (version 0.11) libraries. Survival outcomes were estimated using Kaplan-Meier analysis, and groups were compared with log-rank statistics. Multivariate Cox regression was performed to evaluate the effect of *PIK3CA* gene mutation on survival after adjusting for clinicopathological parameters that included patient age, tumor size, tumor grade, and lymph node status. Hazard ratios and log-rank tests were calculated using the lifelines (version 0.26) library, and  $p < 0.05$  was used as a cut-off for statistical significance. All plots were made using the matplotlib library (version 3.4).

## Results

### PIK3CA mutation is more prevalent in Singapore TNBC

The mutational landscape of TNBC has been reported for three cohorts in the public domain, namely the FUSCC (44), TCGA (12), and the METABRIC (21) cohorts.

A total of 150 Singapore TNBC underwent CGP using the FoundationOne® panel, as previously described (23), to identify somatic mutations (the “SGH” cohort). The mean age of the discovery cohort (57 years) was comparable to that of the three other public datasets under comparison (Supplementary Table 1). In all cohorts, tumor protein P53 (*TP53*) was identified as the most frequently mutated gene, with inactivating mutations in more than 80% of tumors in our cohort (Fig. 1a). Consistent with an observation made by Jiang et al. in their Chinese FUSCC cohort (44), we noticed that *PIK3CA* mutations in our SGH cohort occurred at a significantly higher frequency than in the non-Asian members of the TCGA cohort (Fig. 1b), prompting us to direct our focus on this gene and investigate the clinical and transcriptomic features distinguishing our *PIK3CA*<sup>mut</sup> and *PIK3CA*<sup>WT</sup> tumors. In addition to *PIK3CA*, mutations in breast cancer gene 1 (*BRCA1*), protein tyrosine phosphatase non-receptor type 11 (*PTPN11*), mitogen-activated protein kinase kinase kinase 1 (*MAP3K1*), and

telomerase reverse transcriptase promoter (*TERTp*) were also identified at a significantly higher frequency in our cohort compared to other TNBC cohorts (Fig. 1b, supplementary Table 5).

The 19 *PIK3CA* mutations identified in the SGH cohort corresponded with hotspot mutations known to lead to the constitutive activation of PI3K, such as mutations in the kinase (H1047R; n = 16) or helical (E542K or E545K; n = 3) domains (Table 1). Furthermore, the H1047R mutation, which accounted for half of all *PIK3CA* mutations in both FUSCC and SGH cohorts, was more prevalent in the SGH cohort than the non-Asian TCGA ( $p < 0.05$ ) and primarily Caucasian METABRIC cohorts, but not the FUSCC cohort (Table 1). Targeted sequencing of SGHv cohort revealed similar frequencies for the H1047R mutation (Table 1). In addition, it was also observed that the FUSCC cohort displayed a high frequency of the C2 domain mutation N345K (Supplementary Table 6), a residue ordinarily involved in hydrogen bonding to the p85 subunit of PI3K. These data illustrate that Asian tumors display a particular propensity for acquiring mutations in *PIK3CA* and, therefore, this signaling axis is worthy of further exploration in this population.

Table 1  
Comparison of the PIK3CA CDx hotspot mutations across the TNBC cohorts.

	SGH (n = 117)	FUSCC (n = 276)	FUSCC vs SGH p-val	TCGA (n = 129)	TCGA vs SGH p-val	METABRIC (n = 292)	METABRIC vs SGH p-value	SGHv (n = 50)	SGHv vs SGH p-val
H1047R	16 (13.7%)	29 (10.5%)	0.388	4 (3.1%)	0.004	21 (7.2%)	0.055	4 (8.0%)	0.436
E545K	2 (1.7%)	2 (0.7%)	0.586	1 (0.8%)	0.606	8 (2.7%)	0.731	2 (4.0%)	0.584
H1047L	2 (1.7%)	1 (0.4%)	0.212	0 (0.0%)	0.225	2 (0.7%)	0.324	0 (0.0%)	1
E542K	1 (0.9%)	2 (0.7%)	1	2 (1.6%)	1	5 (1.7%)	0.679	0 (0.0%)	1
E545A	0 (0.0%)	1 (0.4%)	1	0 (0.0%)	1	0 (0.0%)	1	0 (0.0%)	1
Q546R	0 (0.0%)	0 (0.0%)	1	1 (0.8%)	1	0 (0.0%)	1	0 (0.0%)	1
H1047Y	0 (0.0%)	0 (0.0%)	1	1 (0.8%)	1	0 (0.0%)	1	0 (0.0%)	1
C420R	0 (0.0%)	0 (0.0%)	1	0 (0.0%)	1	3 (1.0%)	0.561	0 (0.0%)	1
E545D	0 (0.0%)	0 (0.0%)	1	0 (0.0%)	1	0 (0.0%)	1	0 (0.0%)	1
E545G	0 (0.0%)	0 (0.0%)	1	0 (0.0%)	1	0 (0.0%)	1	0 (0.0%)	1
Q546E	0 (0.0%)	0 (0.0%)	1	0 (0.0%)	1	0 (0.0%)	1	0 (0.0%)	1
<b>Total</b>	<b>21 (17.9%)</b>	<b>35 (12.7%)</b>	<b>0.206</b>	<b>9 (7.0%)</b>	<b>0.011</b>	<b>39 (13.4%)</b>	<b>0.279</b>	<b>6 (12.0%)</b>	<b>0.491</b>

*P-values (p-val) as calculated by the Fisher's exact test. Comparison of non-CDx mutations shown in Online Supplemental Table S5. Abbreviations: SGH, Singapore General Hospital; FUSCC, Fudan University Shanghai Cancer Center; TCGA, The Cancer Genome Atlas.*

### PIK3CA mutation status does not predict clinical outcomes

We next investigated if *PIK3CA* mutations alone could serve as a predictor of clinical outcomes and found that this was not the case in our SGH cohort (Fig. 2a) or the FUSCC (Fig. 2b) or TCGA non-Asian (Fig. 2c) cohorts. However, *PIK3CA* mutations in the METABRIC cohort, which comprised a predominantly Caucasian population, were associated with poorer overall and recurrence-free survival (Fig. 2d). The SGHv cohort results suggested that there was a significantly poorer rate of overall and recurrence-free survival amongst patients with *PIK3CA<sup>mut</sup>* tumors, although this cohort only comprised six *PIK3CA<sup>mut</sup>* tumors (Fig. 2e). Similarly, multivariate analyses adjusting for age and other clinicopathological parameters did not implicate any involvement for *PIK3CA* in the clinical prognoses of the SGH, FUSCC, and METABRIC cohorts (Supplementary Fig. 1).



## PIK3CA mutation is associated with a trend of low immune activity in the SGH cohort

To identify associations between *PIK3CA* mutational status and the immune microenvironment of TNBC tumors, we compared the gene expression levels of T cell markers between *PIK3CA<sup>mut</sup>* and *PIK3CA<sup>WT</sup>* patients. We observed *PIK3CA<sup>mut</sup>* tumors within our cohort to display trends of reduced immune activity (Fig. 3a-d). These findings were further supported by other two public cohorts (Supplementary Fig. 2b-c). Across patients, the gene expression levels of *CD3D* were positively correlated with the cell abundances in the tissue sections (*PIK3CA<sup>mut</sup>*:  $r = 0.58$ ,  $p = 0.0038$ ; *PIK3CA<sup>WT</sup>*:  $r = 0.70$ ;  $p < 0.001$ ) (Fig. 3e). Curiously, while a similar association was observed between *CD8A* expression levels and CD8<sup>+</sup> cell percentages in *PIK3CA<sup>WT</sup>* patients, such an association was absent in *PIK3CA<sup>mut</sup>* patients (Fig. 3f).

Performing the same comparisons in the validation cohort, we observed a similar lower expression level of *CD8A* (Supplementary Fig. 3a), lower CD8 cell numbers (Supplementary Fig. 3b-d), and a positive correlation between *CD3D* gene expression and CD3 cell percentages (Supplementary Fig. 3e). Like in the discovery cohort, *CD8A* gene expression was also correlated with CD8<sup>+</sup> cell abundance in *PIK3CA<sup>WT</sup>* tumors but not *PIK3CA<sup>mut</sup>* tumors (Supplementary Fig. 3f).

Taken together, our discovery and validation cohort data point to a lower T cell presence in *PIK3CA<sup>mut</sup>* tumors and the absence of an association between *CD8A* gene expression and CD8<sup>+</sup> T cell percentages in *PIK3CA<sup>mut</sup>* tumors. These indicate that *CD8A* expression may not be a good surrogate for CD8<sup>+</sup> T cell abundance in patients bearing *PIK3CA* mutations.

## PIK3CA mutation is associated with PD-L1 negativity

To uncover the relationship between *PIK3CA* mutations and reduced tumor immune presence, we compared the tissue expression of PD-L1 between *PIK3CA<sup>mut</sup>* and *PIK3CA<sup>WT</sup>* patients. There was reduced expression of *CD274* (the gene encoding PD-L1) in *PIK3CA<sup>mut</sup>* patients (Fig. 4a) as well as a significantly lower PD-L1 score in *PIK3CA<sup>mut</sup>* patients, as assessed using the SP142 antibody clone (CPS:  $p = 0.020$ , IC:  $p = 0.049$ , TPS:  $p = 0.039$ ) (Fig. 4b). Based on the PD-L1-positivity of  $\geq 1\%$  IC detected by the SP142 antibody, a lower proportion of *PIK3CA<sup>mut</sup>* tumors was classified as PD-L1<sup>+</sup> compared to *PIK3CA<sup>WT</sup>* tumors (Fisher's exact test  $p = 0.094$ ; Fig. 4c). PD-L1 scoring using the 22C3 antibody (positivity indicated by  $\geq 10\%$  CPS) yielded similar results (CPS:  $p = 0.013$ , IC:  $p = 0.065$ , TPS:  $p = 0.021$ ; Fisher's exact test  $p = 0.007$ ) (Fig. 4d-e). The same negative trend between PD-L1 expression and *PIK3CA* mutation was also observed in the SGHv cohort at the RNA and protein levels (Supplementary Fig. 4a-c).

In support of the above results, PD-L1<sup>-</sup> patients of the SGH cohort were observed to possess a higher frequency of *PIK3CA* mutations than PD-L1<sup>+</sup> patients (42.9% compared to 22.7%,  $p = 0.094$  with the SP142 antibody; and 43.2% compared to 16%,  $p = 0.007$  with the 22C3 antibody) (Fig. 4f, Supplementary Table 7). The PD-L1 stratification of patients revealed a difference in the sets of genes most frequently mutated in each stratum, which warrants further investigation (Fig. 4g). Notably, *TERTp* and *MAP3K1* were more frequently mutated in PD-L1<sup>-</sup> patients, with both *MAP3K1* mutations co-occurring with the *PIK3CA* mutations.

## MAPK pathway mutations frequently co-occur with PIK3CA mutations

To identify other mutations associated with *PIK3CA* mutations, the 30 *PIK3CA*<sup>mut</sup> tumors (Fig. 5a) and 87 *PIK3CA*<sup>WT</sup> tumors (Fig. 5b) were sorted according to the presence or absence of other gene mutations. Mutations in *TP53* were found to be significantly less frequent among *PIK3CA*<sup>mut</sup> patients than *PIK3CA*<sup>WT</sup> patients (odds ratio: 0.3), implying a degree of redundancy afforded by the *TP53* mutation, while neurofibromin 1 (*NF1*) was found to be 8.5 times more likely to be mutated in *PIK3CA*<sup>mut</sup> patients compared to *PIK3CA*<sup>WT</sup> patients. Mutations in phosphatase and tensin homolog (*PTEN*) and *PTPN11* occurred exclusively of *PIK3CA* mutations, except in the case of a *PIK3CA*<sup>E109\_I112del</sup> patient who bore mutations in both *PTEN* and *PTPN11*. Similarly, *PIK3R1* mutations occurred largely exclusively of *PIK3CA* mutations, except for a single patient who was also *PIK3CA*<sup>H1047R</sup>. The trends in *PIK3CA* co-mutation and exclusivity were generally recapitulated in the public datasets. Of note, components of the ERK-MAPK pathway appeared to be frequently co-mutated with *PIK3CA* (Fig. 5c, supplementary Table 8).

Integrating selected components of the ERK-MAPK, JNK-MAPK, and PI3K-Akt pathways, the co-mutation and exclusion of mutations with *PIK3CA* suggested a model in which constitutive activation of the PI3K-Akt pathway modulates the ERK-MAPK pathway (Fig. 5d). This was supported by the observation that mutations in the positive regulators of this pathway were gain-of-function, while *NF1*, which is a negative regulator of this pathway, displayed loss-of-function mutations (Supplementary Table 2). In addition, genetic components of the JNK-MAPK pathway, which dampens the PI3K-Akt pathway via IRS1, were often co-mutated with *PIK3CA*, leading to reduced JNK, suggesting that this pathway might co-mutate in *PIK3CA*<sup>mut</sup> tumors to overcome feedback regulation.

## Discussion

Given that PI3K dysregulation is highly associated with the development of resistance to current standard-of-care treatments in breast cancer patients (15), and that the role of *PIK3CA* in TNBC is still largely controversial and inconclusive, our study was designed to assess its role within the tumor immune microenvironment of TNBCs. In our cohort of TNBCs, we demonstrated a higher prevalence of *PIK3CA* mutations which was associated with negative PD-L1 expression, suggesting a role to prioritize targeting of this pathway in PD-L1<sup>-</sup> TNBCs. This was concluded based on a comparison with other distinct cohorts using publicly accessible data. Our results demonstrated that the associations among PD-L1 negativity and *PIK3CA* alterations were valid in both the clinically relevant PD-L1 clones (SP142 and 22C3) using the respective parameters and cut-offs, which support a previous report of a correlation between *PIK3CA* alteration and PD-L1 negativity (45).

A study by Jiang et al. based on The Cancer Genome Atlas (TCGA) showed *PIK3CA* mutations to be more frequent in Chinese than Caucasian patients with TNBC, though statistical significance was not achieved when they included African American patients in the analysis (22). However, the clinical significance of such differences in the Asian population has not yet been characterized. This study is the first to highlight the high prevalence of *PIK3CA* mutations in Singapore TNBC, regionally representing Southeast Asia, especially when compared to cohorts of East Asian and African American populations. Collectively, *PIK3CA*, *TP53*, *BRCA1*, *PTPN11*, and *MAP3K1* mutations were also found to have a higher prevalence, emphasizing on the need for further studies into the relevant mechanisms.

One limitation of our study is that we included only early stage TNBC. However, it is still unclear whether the rates of *PIK3CA* mutations in TNBC can vary significantly according to disease stage and ethnicity. Jiang et al. reported comparable rates of primary and metastatic TNBC *PIK3CA* alterations in an East Asian cohort (44), whereas Mosele et al. reported better clinical outcomes for *PIK3CA<sup>mut</sup>* metastatic TNBC (46) that were not seen in all the primary TNBC cohorts that we analyzed, such as the Southeast Asian cohort. In fact, the METABRIC cohort showed the opposite results. However, in both the primary and metastatic settings, the impact of *PIK3CA* mutations on clinical outcomes might vary substantially. Multiple inhibitors targeting the PI3K/AKT/mTOR pathway entered late phase clinical trials in TNBC. An AKT inhibitor, capivasertib, has been tested in combination with paclitaxel in a phase II trial for untreated metastatic TNBC, and it achieved significantly longer progression-free survival and overall survival among patients (47). Similarly, the addition of AKT inhibitor, ipatasertib, to paclitaxel in a phase II study also improved progression-free survival compared to paclitaxel alone in metastatic TNBC patients, particularly in tumors with *PIK3CA* mutation (48). However, according to results from the phase III study, the above combination failed to improve progression-free survival in *PIK3CA/AKT/PTEN*-altered TNBCs (49). The above-mentioned example of a failed phase III study despite promising result from phase II study depicts the challenges faced in developing novel therapeutic strategies for PI3K-altered TNBC. Further understanding of *PIK3CA* mutations in TNBC is therefore vital for the development of PI3K inhibitors as treatment options.

Apart from the direct proliferative effects of PI3K pathway on tumor cells, it has also been suggested that the pathway is involved in initiating an immunosuppressive microenvironment (50, 51). PI3K activation and signaling mediates an immunosuppressive phenotype in myeloid cells, enhances the function of regulatory T cells, decrease CD8 T cell infiltration, and impair its cytotoxicity (50, 51). This might partially explain our observation that by comparing both the RNA and cellular levels of the immune cells, we found that, while CD8 T cell abundance was correlated with CD8 RNA levels in *PIK3CA<sup>WT</sup>* tumors, this association was absent from *PIK3CA<sup>mut</sup>* tumors. This is consistent with studies describing the negative regulator role of *PIK3CA* in cell fate decision (52–54). As such, the use of mono-therapeutic PI3K inhibitors alone could potentially alleviate the immunosuppression. In terms of combination therapy, a recent success in combining immune checkpoint blockade with a PI3K inhibitor (alpelisib) has been reported for breast cancer patients (15).

Based on this study, we found that *PIK3CA* alterations were often associated with PD-L1 (SP142 and 22C3) negativity, which raise the potential of *PIK3CA* as a negative biomarker selecting patients less suited for immune checkpoint inhibition and the development of PI3K/AKT pathway inhibitors perhaps to be included in adjuvant therapy for high-risk residual TNBC. In metastatic TNBC, researchers did not find any correlation between PD-L1 expression and mutations in *PIK3CA* (46), which suggests that PI3K inhibitors could be independently developed from drugs targeting PD-L1.

Lastly, while the trends in *PIK3CA* co-mutation and exclusivity were generally recapitulated in the public datasets, our study also described a high frequency of *PIK3CA* and *MAP3K1* co-mutation in TNBC patients. A separate study of *PIK3CA<sup>mut</sup>* metastatic breast cancer patients (CT02299999) found that *PIK3CA* mutations were similarly associated with a higher frequency of *MAP3K1* mutations, but they occurred mutually exclusively of AKT serine/threonine kinase 1 (*AKT1*) mutations (46). As changes to *PIK3CA*, *MAP3K1*, *AKT1*, and *PTEN* have all been correlated with those who clinically benefit from PI3K inhibitor treatments (46, 55), genomic

testing for the abovementioned genes might be important in development of PI3K/AKT pathway inhibitors in the context of early TNBC.

In conclusion, our study demonstrated a high prevalence of *PIK3CA*, *TP53*, *BRCA1*, *PTPN11*, and *MAP3K1* alterations in our Singapore cohort of TNBC, and that *PIK3CA* alterations were often associated with low PD-L1 expression. The mechanism through which the *PIK3CA* mutations impact the TNBC immune microenvironment warrants further study in a larger and multi-centered cohort for validation, which may provide alternative, effective strategies for breast cancer clinical management.

## Declarations

**Acknowledgements:** Not applicable.

**Conflict of Interest:** Dr Tira Tan; (i) Personal interests with Astra Zeneca, DHPL Malaysia SDN MHD, DKSH, Everest Medicines (Singapore) Pte Ltd, MSD, Novartis, Pfizer and Roche, (ii) Financial interests with AstraZeneca, Daiichi Sankyo, Genentech, Novartis, Odonate, Roche and Sanofi, and (iii) Non-financial interest with ASCO. Dr. Rebecca Dent; (i) Advisor/Consultant to AstraZeneca, Eisai, MSD, Novartis, Pfizer and Roche, (ii) Travel, accommodations and expenses paid for by Eisai, MSD, Pfizer and Roche, and (iii) Research interest with AstraZeneca and Roche. The remaining authors declare that they have no competing interest.

**Ethics approval:** The Centralized Institutional Review Board of SingHealth provided ethical approval for the use of patient materials in this study (CIRB ref.: 2013/664/F and 2015/2199). Written informed consent is not required for deidentified subjects in Singapore.

**Author Contributions:** The study was designed and directed by T.B.T., R.A.D. and T.P.H., and coordinated by J.Y., J.Y., V.K., J.C.T.L. and C.R.J. acquired the data. The analysis was done by B.T., J.F.Y. and M.C.L.. J.Y., H.S., C.N., J.I., T.B.T. and T.P.H. provided advice from pathology perspectives. R.A.D. provided advice from clinical perspectives. J.Y., D.G., T.T. drafted the manuscript, which was commented on and revised by all authors. All authors read and approved the final manuscript.

**Funding:** This project was funded by Singapore National Medical Research Council (MOH-000323-00, OFYIRG19may-0007) and Singapore General Hospital Centre Grant (CG) (NMRC/CG/M011/2017\_SGH).

**Data Availability:** Data can be obtained from the corresponding authors upon request.

## References

1. Yeong J, Thike AA, Ikeda M, Lim JCT, Lee B, Nakamura S, et al. Caveolin-1 expression as a prognostic marker in triple negative breast cancers of Asian women. *Journal of clinical pathology*. 2018;71(2):161–7.
2. Gole L, Yeong J, Lim JCT, Ong KH, Han H, Thike AA, et al. Quantitative stain-free imaging and digital profiling of collagen structure reveal diverse survival of triple negative breast cancer patients. *Breast Cancer Research*. 2020;22:1–13.
3. Matsumoto H, Thike AA, Li H, Yeong J, Koo S-I, Dent RA, et al. Increased CD4 and CD8-positive T cell infiltrate signifies good prognosis in a subset of triple-negative breast cancer. *Breast cancer research and treatment*. 2016;156(2):237–47.

4. Seow DYB, Yeong JPS, Lim JX, Chia N, Lim JCT, Ong CCH, et al. Tertiary lymphoid structures and associated plasma cells play an important role in the biology of triple-negative breast cancers. *Breast Cancer Research and Treatment*. 2020;1–9.
5. Yeong J, Lim JCT, Lee B, Li H, Ong CCH, Thike AA, et al. Prognostic value of CD8 + PD-1 + immune infiltrates and PDCD1 gene expression in triple negative breast cancer. *Journal for immunotherapy of cancer*. 2019;7(1):34.
6. Yeong J, Lim JCT, Lee B, Li H, Chia N, Ong CCH, et al. High Densities of Tumor-Associated Plasma Cells Predict Improved Prognosis in Triple Negative Breast Cancer. *Front Immunol*. 2018;9:1209-.
7. Chan JJ, Tan TJY, Dent RA. Are There Any Clinically Relevant Subgroups of Triple-Negative Breast Cancer in 2018? *Journal of Oncology Practice*. 2018;14(5):281–9.
8. Lai CPT, Yeong JPS, Tan AS, Ong CHC, Lee B, Lim JCT, et al. Evaluation of phospho-histone H3 in Asian triple-negative breast cancer using multiplex immunofluorescence. *Breast cancer research and treatment*. 2019;178(2):295–305.
9. Yeong J, Thike AA, Lim JCT, Lee B, Li H, Wong S-C, et al. Higher densities of Foxp3 + regulatory T cells are associated with better prognosis in triple-negative breast cancer. *Breast cancer research and treatment*. 2017;163(1):21–35.
10. Vanhaesebroeck B, Stephens L, Hawkins P. PI3K signalling: the path to discovery and understanding. *Nature Reviews Molecular Cell Biology*. 2012;13(3):195–203.
11. Banerji S, Cibulskis K, Rangel-Escareno C, Brown KK, Carter SL, Frederick AM, et al. Sequence analysis of mutations and translocations across breast cancer subtypes. *Nature*. 2012;486(7403):405–9.
12. Koboldt DC, Fulton RS, McLellan MD, Schmidt H, Kalicki-Veizer J, McMichael JF, et al. Comprehensive molecular portraits of human breast tumours. *Nature*. 2012;490(7418):61–70.
13. Kalinsky K, Jacks LM, Heguy A, Patil S, Drobnjak M, Bhanot UK, et al. PIK3CA Mutation Associates with Improved Outcome in Breast Cancer. *Clinical Cancer Research*. 2009;15(16):5049.
14. Zardavas D, te Marvelde L, Milne RL, Fumagalli D, Fountzilias G, Kotoula V, et al. Tumor PIK3CA Genotype and Prognosis in Early-Stage Breast Cancer: A Pooled Analysis of Individual Patient Data. *Journal of Clinical Oncology*. 2018;36(10):981–90.
15. Zhang Z, Richmond A. The Role of PI3K Inhibition in the Treatment of Breast Cancer, Alone or Combined With Immune Checkpoint Inhibitors. *Front Mol Biosci*. 2021;8:648663.
16. Bai J, Gao Z, Li X, Dong L, Han W, Nie J. Regulation of PD-1/PD-L1 pathway and resistance to PD-1/PD-L1 blockade. *Oncotarget*. 2017;8(66):110693–707.
17. Yeong J, Lim JCT, Lee B, Li H, Ong CCH, Thike AA, et al. Prognostic value of CD8 + PD-1 + immune infiltrates and PDCD1 gene expression in triple negative breast cancer. *Journal for ImmunoTherapy of Cancer*. 2019;7(1):34.
18. Matsumoto H, Thike AA, Li H, Yeong J, Koo SL, Dent RA, et al. Increased CD4 and CD8-positive T cell infiltrate signifies good prognosis in a subset of triple-negative breast cancer. *Breast Cancer Res Treat*. 2016;156(2):237–47.
19. Yeong J, Thike AA, Lim JC, Lee B, Li H, Wong SC, et al. Higher densities of Foxp3(+) regulatory T cells are associated with better prognosis in triple-negative breast cancer. *Breast Cancer Res Treat*. 2017;163(1):21–35.

20. Lakhani S, Ellis I, Schnitt S, Tan P, van de Vijver M. World Health Organization classification of tumours. WHO classification of tumors in the breast. 2012;4.
21. Curtis C, Shah SP, Chin SF, Turashvili G, Rueda OM, Dunning MJ, et al. The genomic and transcriptomic architecture of 2,000 breast tumours reveals novel subgroups. *Nature*. 2012;486(7403):346–52.
22. Jiang YZ, Ma D, Suo C, Shi J, Xue M, Hu X, et al. Genomic and Transcriptomic Landscape of Triple-Negative Breast Cancers: Subtypes and Treatment Strategies. *Cancer cell*. 2019;35(3):428 – 40.e5.
23. Frampton GM, Fichtenholtz A, Otto GA, Wang K, Downing SR, He J, et al. Development and validation of a clinical cancer genomic profiling test based on massively parallel DNA sequencing. *Nature biotechnology*. 2013;31(11):1023–31.
24. Ross JS, Fakih M, Ali SM, Elvin JA, Schrock AB, Suh J, et al. Targeting HER2 in colorectal cancer: The landscape of amplification and short variant mutations in ERBB2 and ERBB3. *Cancer*. 2018;124(7):1358–73.
25. Bolger AM, Lohse M, Usadel B. Trimmomatic: a flexible trimmer for Illumina sequence data. *Bioinformatics*. 2014;30(15):2114–20.
26. Li H, Durbin R. Fast and accurate long-read alignment with Burrows-Wheeler transform. *Bioinformatics*. 2010;26(5):589–95.
27. Li H, Handsaker B, Wysoker A, Fennell T, Ruan J, Homer N, et al. The Sequence Alignment/Map format and SAMtools. *Bioinformatics (Oxford, England)*. 2009;25(16):2078–9.
28. Garrison EP, Marth GT. Haplotype-based variant detection from short-read sequencing. *arXiv: Genomics*. 2012.
29. McLaren W, Gil L, Hunt SE, Riat HS, Ritchie GRS, Thormann A, et al. The Ensembl Variant Effect Predictor. *Genome Biology*. 2016;17(1):122.
30. Sherry ST, Ward MH, Kholodov M, Baker J, Phan L, Smigielski EM, et al. dbSNP: the NCBI database of genetic variation. *Nucleic Acids Res*. 2001;29(1):308–11.
31. Tate JG, Bamford S, Jubb HC, Sondka Z, Beare DM, Bindal N, et al. COSMIC: the Catalogue Of Somatic Mutations In Cancer. *Nucleic Acids Res*. 2019;47(D1):D941-d7.
32. Landrum MJ, Lee JM, Benson M, Brown G, Chao C, Chitipiralla S, et al. ClinVar: public archive of interpretations of clinically relevant variants. *Nucleic Acids Res*. 2016;44(D1):D862-8.
33. Thorvaldsdóttir H, Robinson JT, Mesirov JP. Integrative Genomics Viewer (IGV): high-performance genomics data visualization and exploration. *Briefings in Bioinformatics*. 2012;14(2):178–92.
34. Yeong J, Thike AA, Lim JC, Lee B, Li H, Wong SC, et al. Higher densities of Foxp3 + regulatory T cells are associated with better prognosis in triple-negative breast cancer. *Breast cancer research and treatment*. 2017;23(10):017–4161.
35. Yeong J, Lim JCT, Lee B, Li H, Chia N, Ong CCH, et al. High Densities of Tumor-Associated Plasma Cells Predict Improved Prognosis in Triple Negative Breast Cancer. *Frontiers in Immunology*. 2018;9(1209).
36. Sun WY, Lee YK, Koo JS. Expression of PD-L1 in triple-negative breast cancer based on different immunohistochemical antibodies. *Journal of Translational Medicine*. 2016;14(1):173.
37. Karnik T, Kimler BF, Fan F, Tawfik O. PD-L1 in breast cancer: comparative analysis of 3 different antibodies. *Human Pathology*. 2018;72:28–34.

38. Yeong J, Tan T, Chow ZL, Cheng Q, Lee B, Seet A, et al. Multiplex immunohistochemistry/immunofluorescence (mIHC/IF) for PD-L1 testing in triple-negative breast cancer: a translational assay compared with conventional IHC. *Journal of Clinical Pathology*. 2020;73(9):557.
39. Lim JCT, Yeong JPS, Lim CJ, Ong CCH, Wong SC, Chew VSP, et al. An automated staining protocol for seven-colour immunofluorescence of human tissue sections for diagnostic and prognostic use. *Pathology*. 2018;50(3):333–41.
40. Ng HHM, Lee RY, Goh S, Tay ISY, Lim X, Lee B, et al. Immunohistochemical scoring of CD38 in the tumor microenvironment predicts responsiveness to anti-PD-1/PD-L1 immunotherapy in hepatocellular carcinoma. *J Immunother Cancer*. 2020;8(2).
41. Tien TZ, Lee J, Lim JCT, Chen XY, Thike AA, Tan PH, et al. Delineating the breast cancer immune microenvironment in the era of multiplex immunohistochemistry/immunofluorescence. *Histopathology*. 2021;79(2):139–59.
42. Salgado R, Denkert C, Demaria S, Sirtaine N, Klauschen F, Pruneri G, et al. The evaluation of tumor-infiltrating lymphocytes (TILs) in breast cancer: recommendations by an International TILs Working Group 2014. *Annals of Oncology*. 2015;26(2):259–71.
43. Laksameethanasan D, Tan R, Toh G, Loo L-H. cellXpress: a fast and user-friendly software platform for profiling cellular phenotypes. *BMC Bioinformatics*. 2013;14 Suppl 16(Suppl 16):S4-S.
44. Jiang Y-Z, Liu Y, Xiao Y, Hu X, Jiang L, Zuo W-J, et al. Molecular subtyping and genomic profiling expand precision medicine in refractory metastatic triple-negative breast cancer: the FUTURE trial. *Cell Research*. 2020.
45. Huang RSP, Li X, Haberberger J, Sokol E, Severson E, Duncan DL, et al. Biomarkers in Breast Cancer: An Integrated Analysis of Comprehensive Genomic Profiling and PD-L1 Immunohistochemistry Biomarkers in 312 Patients with Breast Cancer. *The oncologist*. 2020;25(11):943–53.
46. Mosele F, Stefanovska B, Lusque A, Tran Dien A, Garberis I, Droin N, et al. Outcome and molecular landscape of patients with PIK3CA-mutated metastatic breast cancer. *Annals of oncology: official journal of the European Society for Medical Oncology*. 2020;31(3):377–86.
47. Schmid P, Abraham J, Chan S, Wheatley D, Brunt AM, Nemsadze G, et al. Capivasertib Plus Paclitaxel Versus Placebo Plus Paclitaxel As First-Line Therapy for Metastatic Triple-Negative Breast Cancer: The PAKT Trial. *Journal of Clinical Oncology*. 2019;38(5):423–33.
48. Kim S-B, Dent R, Im S-A, Espi e M, Blau S, Tan AR, et al. Ipatasertib plus paclitaxel versus placebo plus paclitaxel as first-line therapy for metastatic triple-negative breast cancer (LOTUS): a multicentre, randomised, double-blind, placebo-controlled, phase 2 trial. *Lancet Oncol*. 2017;18(10):1360–72.
49. Rebecca Dent, Sung-Bae Kim, Mafalda Oliveira, Carlos Barrios, Joyce O’Shaughnessy, Steven J Isakoff, et al. Double-blind placebo (PBO)-controlled randomized phase III trial evaluating first-line ipatasertib (IPAT) combined with paclitaxel (PAC) for PIK3CA/AKT1/PTEN-altered locally advanced unresectable or metastatic triple-negative breast cancer (aTNBC): primary results from IPATunity130 Cohort A. 2020 San Antonio Breast Cancer Virtual Symposium; San Antonio, Texas: Cancer Research; 2021.
50. Aydin E, Faehling S, Saleh M, Llao Cid L, Seiffert M, Roessner PM. Phosphoinositide 3-Kinase Signaling in the Tumor Microenvironment: What Do We Need to Consider When Treating Chronic Lymphocytic Leukemia With PI3K Inhibitors? *Front Immunol*. 2020;11:595818.

51. Sun P, Meng L-h. Emerging roles of class I PI3K inhibitors in modulating tumor microenvironment and immunity. *Acta Pharmacologica Sinica*. 2020;41(11):1395–402.
52. Wentink MWJ, Mueller YM, Dalm VASH, Driessen GJ, van Hagen PM, van Montfrans JM, et al. Exhaustion of the CD8 + T Cell Compartment in Patients with Mutations in Phosphoinositide 3-Kinase Delta. *Frontiers in Immunology*. 2018;9.
53. Singh MD, Ni M, Sullivan JM, Hamerman JA, Campbell DJ. B cell adaptor for PI3-kinase (BCAP) modulates CD8 + effector and memory T cell differentiation. *Journal of Experimental Medicine*. 2018;215(9):2429–43.
54. Murter B, Kane LP. Control of T lymphocyte fate decisions by PI3K signaling. *F1000Res*. 2020;9:F1000 Faculty Rev-171.
55. Schmid P, Abraham J, Chan S, Wheatley D, Brunt AM, Nemsadze G, et al. Capivasertib Plus Paclitaxel Versus Placebo Plus Paclitaxel As First-Line Therapy for Metastatic Triple-Negative Breast Cancer: The PAKT Trial. *Journal of Clinical Oncology*. 2020;38(5):423–33.

## Supplementary Files

This is a list of supplementary files associated with this preprint. Click to download.

- [Supptable1.docx](#)
- [SuppTable2.docx](#)
- [Supptable3.docx](#)
- [SuppTable4.docx](#)
- [SuppTable5.docx](#)
- [SuppTable6.docx](#)
- [SuppTable7.docx](#)
- [SuppTable8.docx](#)
- [Suppfig1.jpg](#)
- [Suppfig2.jpg](#)
- [Suppfig3.jpg](#)
- [Suppfig4.jpg](#)